ACS APPLIED MATERIALS & INTERFACES

Research Article

www.acsami.org

A Systematic Investigation of Polymer Binder Flexibility on the Electrode Performance of Lithium-Ion Batteries

Neslihan Yuca,[†,‡] Hui Zhao,[†] Xiangyun Song,[†] Murat Ferhat Dogdu,[‡] Wen Yuan,[†] Yanbao Fu,[†] Vincent S. Battaglia,[†] Xingcheng Xiao,[§] and Gao Liu*[,†]

[†]Environmental Energy Technologies Division, Lawrence Berkeley National Laboratory, Berkeley, California 94720, United States

[‡]Istanbul Technical University, Energy Institute Istanbul 34469, Turkey

[§]Global Research & Development Center, General Motors, Warren, Michigan 48090, United States

Supporting Information

ABSTRACT: The mechanical failure at the electrode interfaces (laminate/current collector and binder/particle interfaces) leads to particle isolation and delamination, which has been regarded as one of the main reasons for the capacity decay and cell failure of lithium-ion batteries (LIBs). Polymer binder provides the key function for a good interface property and for maintaining the electrode integrity of LIBs. Triethylene glycol monomethyl ether (TEG) moieties were incorporated into polymethacrylic acid (PMAA) to different extents at the molecular level. Microscratch tests of the graphite electrodes based on these binders indicate that the electrode is more flexible with 5 or 10% TEG in the polymer binders. Crack generation is inhibited by the flexible TEG-containing binder, compared to that of the unmodified PMAA-based electrode, leading to the better cycling performance of the flexible electrode. With a 10% TEG moiety in the binder, the graphite half-cell reaches a reversible capacity of >270 mAh/g at the 1C rate, compared to a value of ~190 mAh/g for the unmodified PMAA binder.

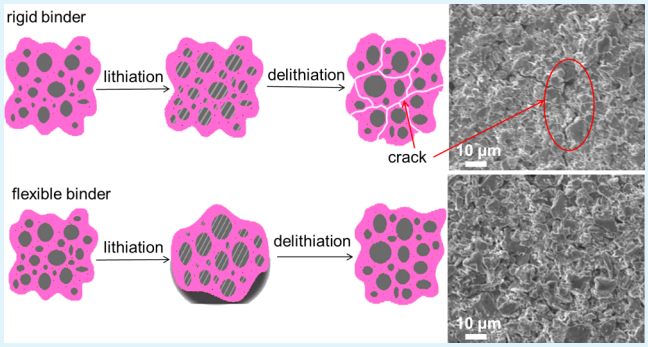

KEYWORDS: *polymer binder, flexibility, graphite anode, lithium-ion battery*

1. INTRODUCTION

Among the energy storage devices,[1,2] rechargeable lithium-ion batteries (LIBs) are widely used as power sources for portable electronics and more recently have been used for electrical vehicles and electrical grid storage.[3] The wide application of LIBs has boosted the development of novel materials and systems for enhancing the energy density and cycle life of LIBs. In a conventional electrode laminate of LIBs, polymer binders are inactive but indispensable components.[4] Polymer binders, such as polyvinylidene fluoride (PVDF), hold the active materials and conductive additives mechanically in the electrode laminate. Electronically conductive additives, such as acetylene black (AB), are used to allow electrical conductivity throughout the electrode. The combined polymer binder and conductive additives maintain the mechanical and electronic integrity of the entire electrode. In addition, the polymer binders coat the active material surfaces, so the polymer swells in the electrolyte to provide ionic conductivity.[5] The mechanical failure at the electrode interfaces (laminate/current collector and binder/particle interfaces) leads to particle isolation and delamination, which has been regarded as one of the main reasons for the capacity decay and cell failure of LIBs.[6−9] Lee and co-workers introduced a conductive adhesive layer between the current collector and the active material layer, and an improved cycling performance was observed for both graphite or graphite/silicon electrodes.[10] Typically, LIB electrodes rely on polymer binders to attain particle/particle cohesion and electrode laminate/current collector adhesion.[11] An optimized design of polymer binders should be able to eliminate crack generation in the electrode,[12] and the development of a suitable binder is becoming an important part of the solution to allow the stable cycling of novel electrode active materials, such as high-capacity alloy anodes (silicon[13] and tin[14,15]) and high-voltage cathodes.[16,17] The state-of-the-art roll-to-roll lamination process in industry[18] also specifically requires a flexible and ductile nature of the polymer binders and electrode, which helps to prevent crack generation and delamination during processing. Incorporation of triethylene glycol monomethyl ether (TEG) moieties in the polymer is supposed to increase both the interface adhesion and the ductility to better eliminate stress-induced fracture.[19,20] In fact, poly(ethylene oxide) (PEO) is known to form a stable interface layer between lithium metal and the PEO electrolyte; thus, it is chemically suitable in the anode environment.[21]

Received: July 21, 2014
Accepted: September 9, 2014
Published: September 9, 2014

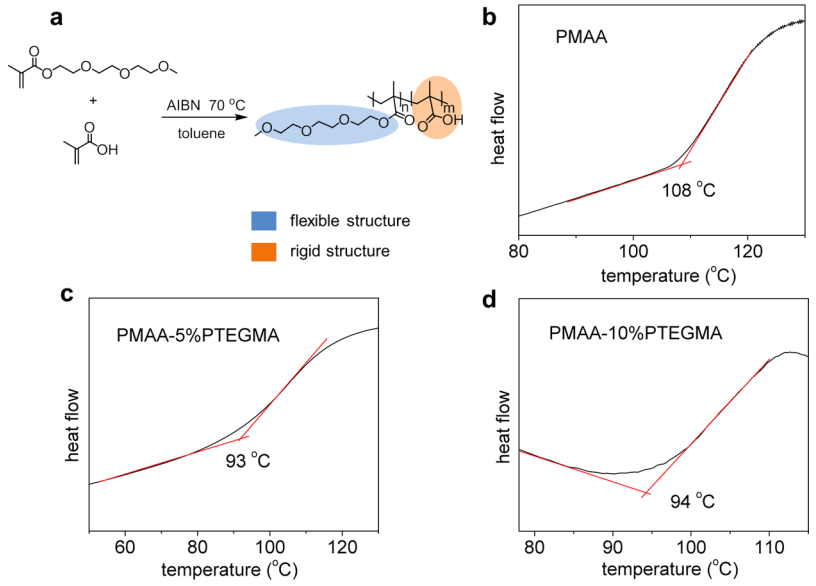

Figure 1. (a) Synthetic route for the TEG-containing polymethacrylic acid (PMAA) polymers, with flexible and rigid structures highlighted. (b–d) Differential scanning calorimetry curves of PMAA, PMAA-5% PTEGMA, and PMAA-10% PTEGMA, respectively, indicating the glass transition temperatures (T_g) of different polymers.

To unveil the role of the polymer binders in the inhibition of failure of electrode interfaces, a rigid polymer binder was chemically modified to gradually improve the flexibility. Different binders were used to fabricate electrode laminates. Microscratch tests were conducted at the surface of the electrodes to reveal the different mechanical responses from the electrode made with the rigid binder and flexible binder. Graphite electrodes assembled using the modified flexible binder can inhibit the generation of cracks, leading to improved cell cycling performance.

2. RESULTS AND DISCUSSION

2.1. Synthesis of the PMAA-Based Polymer Binders. We use poly(methacrylic acid) (PMAA) as model polymer binder, which offers a high concentration of functional groups (one carboxylic acid group in each repeating unit) and allows facile structural modification via copolymerization.[22] There are several reasons that PMAA was used as the polymer binder to study the influence of TEG in this study. Polymers such as PMAA and poly(acrylic acid) (PAA) with a high concentration of acid functionality gain wide application as polymer binders for LIBs.[23,24] However, the negative side of this structure is that PMAA- and PAA-based electrode laminates are rigid and brittle, which easily undergo delamination during the roll-to-roll electrode handling in industry.[25] Also, because of the high concentration of carboxylic acid groups, PAA- and PMAA-based electrodes tend to absorb large amounts of water and ultimately lead to swelling of cells (gas generation) during the course of use, thus, modification of the PMAA and reduction of the amount of acid functional groups are advantageous. Ethylene glycol-based polymers have been intensively investigated as solid-state electrolytes for several decades,[26] yet the use of pure poly(ethylene glycol) (PEG) as a polymer binder seems to be less attractive.[27] PEG has a high solubility in carbonate-based electrolytes, and this should lead to an uncontrolled swelling of the electrode in the electrolyte, which will lead to the loss of the electrical contact between the active materials and the electrode.[23] However, instead of using pure PEG polymer as a binder, our recent result indicates an advantage of incorporating an ethylene glycol structure to modify the binder property. A balanced multifunctionality with high electronic conductivity, mechanical adhesion, ductility, and electrolyte uptake was realized via modification using ethylene glycol,[28] and a full-capacity alloy anode was thus obtained on the basis of this new binder. There are several advantages a binder could gain from an ethylene glycol structural moiety. Because of the good lithium-ion conductivity and the solubility with carbonate-based electrolytes, polymer binders modified by ethylene glycol have a good electrolyte uptake property, which facilitates the transport of lithium ion between electrolytes and electrode active materials. As a polymer segment with a low glass transition temperature (T_g, at approximately −60 °C), ethylene glycol allows a more ductile nature of the polymer binder, and triethylene glycol methacrylate (TEGMA) is chosen as a comonomer (Figure 1a) to bring the ethylene glycol moiety into the polymer binder. The methacrylate structure in this monomer allows copolymerization chemistry with MAA (Figure 1a), and a uniform distribution of TEGMA in the final polymer binder is achieved. Incorporation of TEG structure into the polymer allows us to systematically investigate the influence of the mechanical properties of the binder when it is used in LIBs. A typical free radical polymerization is conducted using azobisisobutylonitrile (AIBN) as an initiator and toluene as a solvent. The reaction was performed at 70 °C for ∼24 h before precipitation in hexane to remove residual monomers. Three different copolymers were synthesized in the lab, with 0, 5, or 10 wt % TEGMA monomers, and the final polymers were labeled PMAA, PMAA-5% PTEGMA, and PMAA-10% PTEGMA. The T_g values of the different polymers were characterized using a differential scanning calorimeter, as shown in panels b and c of Figure 1. PMAA has a T_g of ∼108 °C, which is consistent with the value in the literature. Even with a small amount of the PTEGMA component (5%), T_g is lowered to 93 °C (Figure 1c), and this value does not change much [94 °C (Figure 1d)] when the level of PTEGMA is increased to 10%. The lowered

glass transition temperature indicates a more flexible nature with the incorporation of PTEGMA structure.

The structures are confirmed by the ^{1}H nuclear magnetic resonance (NMR) spectra shown in Figure 2. The doublet at

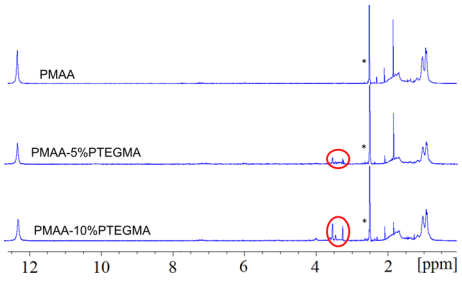

Figure 2. ^{1}H nuclear magnetic resonance spectra of PMAA-based binders collected in d_6-DMSO, with asterisks marking the solvent signals arising from the proton residuals due to incomplete deuteration and the signals corresponding to TEG highlighted.

0.9−1.1 ppm is clear evidence of the polymerized methacrylate polymer, corresponding to the CH_3-C(CH_2)- substructure. While the singlet at 12.4 ppm represents the carboxylic acid proton in PMAA, the broad signal between 1.6 and 2.1 ppm is assigned to the -CH_2-C(CH_3)- substructure in the polymer backbone. The successful incorporation of TEG structure into the synthesized polymer binder is corroborated by the signals between 3.3 and 3.6 ppm, which corresponds to the -CH_2-CH_2-O- substructure in the TEG side chain.

A high molecular weight is a prerequisite for a good mechanical and binding property, which is stringently required for a polymer binder. Gel permeation chromatography (GPC) was used to characterize the molecular weight and polydispersity index (PDI) of the PMAA-based polymers with different TEG contents, as shown in Table 1. The three different polymers have molecular weights of >200000 Da. The relatively large PDI of ∼2.0 is typical for a free radical polymerization.

Table 1. Molecular Weights and PDIs of the Synthesized PMAA-Based Polymer Binder

	M_n	M_w	PDI
PMAA	220000	440000	2.0
PMAA-5% PTEGMA	230000	470000	2.0
PMAA-10% PTEGMA	210000	460000	2.2

2.2. Physical Properties of the Polymers and Electrodes. A microscratch test[29] was conducted on the pristine electrode samples using the PMAA-based polymers to study the influence of TEG on the mechanical properties of the laminates, as shown in panels a and b of Figure 3. A composite electrode model proposed recently by Qi and Li[11] was used to explain the microscratch test results. In the microscratch test, the force applied to the microindenter tip gradually increased; thus, in a rigid polymer like PMAA, the particles were pushed onto the sides and the tip gradually goes down into the electrode laminate to give a negative scratch depth. For compliant polymers, on the other hand, particle/particle cohesion was stronger and the particles were difficult to push onto the sides. As the microindenter tip started to plow, the particles accumulated in front of the diamond tip. This tends to lift up the microindenter tip. The final scratch depth is ∼0 for PMAA-5% PTEGMA, and the diamond tip was even pushed upward for PMAA-10% PTEGMA, giving a positive scratch depth. Many polymer binders for LIBs, such as poly(acrylic acid) (PAA), polymethacrylic acid (PMAA), and carboxymethyl cellulose (CMC), have high Young's moduli (elastic moduli). Electrode laminates based on these rigid binders tend to generate cracks under high-stress conditions, leading to laminate/current collector delamination and particle/particle isolation, and it becomes more serious for the high-capacity alloy anodes.[30] The TEG structural moiety in the polymer binders permits a more compliant nature, which could better accommodate the change in volume of the active material, and less stress will accumulate in the binder, as well as at the interface between the binder and the active materials.

The coefficient of friction (COF) in the scratch test reflects the composite nature of the electrode and the mechanical properties of the polymer binder. As shown in Figure 3b, the PMAA laminate shows behavior similar to that of PVDF-based graphite laminate, and the COF increases rapidly with an increasing normal load because the microindenter tip plowed and slid on the electrode surface. A further increase in the normal load allowed a steady state of the COF. TEG-containing polymer binders, on the other hand, exhibited a higher COF from the initial stage of the test; this is consistent with their more compliant and greater binding strength, which leads to stronger interaction with the polar diamond tip used in the tests. The morphologies of the electrode after the scratch test indicate an obvious difference, as shown in panels d−f of Figure 3. A rigid polymer like PMAA was pushed away to the sides by the tip during scratch test, and a clear scratch track is shown. With greater TEG content in the polymer, the binder becomes more ductile and the scratch track becomes less obvious. In the case of the PMAA-10% PTEGMA-based laminate, it is even difficult to see the scratch track via scanning electron microscopy (SEM). A scratch test simulates the stress induced by the volume change of the electrode active material; this result essentially indicates that more flexible binders such as PMAA-5% PTEGMA and PMAA-10% PTEGMA provide a higher tolerance of the change in volume through its optimized ductility.[31,32] Note that this property is especially important for the recent development of high-capacity alloy anodes for LIBs.[33]

The improvement in the flexibility of the polymer was also corroborated by the adhesion tests in Figure 3c.[34] As shown in the microscratch test, a brittle polymer binder like PMAA provides a weak particle/particle cohesion strength, which results in a weak load transfer capability. This explains the peel test behavior of the PMAA laminate. A small peel-off work load (∼2 N) was shown initially; as the testing proceeded, this value fluctuated until an electrode failed. As a more compliant polymer binder is supposed to significantly strengthen the mechanical binding force and enhance the particle/particle cohesion strength, the peel-off work load started with a high value (∼5 N for PMAA-5% PTEGMA and ∼7 N for PMAA-10% PTEGMA), confirming this high cohesion strength. Introduction of a TEG structural moiety successfully enhanced the adhesion force, and this enhancement was more obvious with greater TEG content in the binder.

2.3. Electrochemical Performance. To assess the electrochemical stability of the polymer, cyclic voltammetry (CV) of the different binders was performed, as shown in Figure 4. The working electrode was a copper foil coated with a polymer film without graphite, using lithium foil as the counter and reference electrode with EC/DEC and 1 M $LiPF_6$ as the electrolyte.[4]

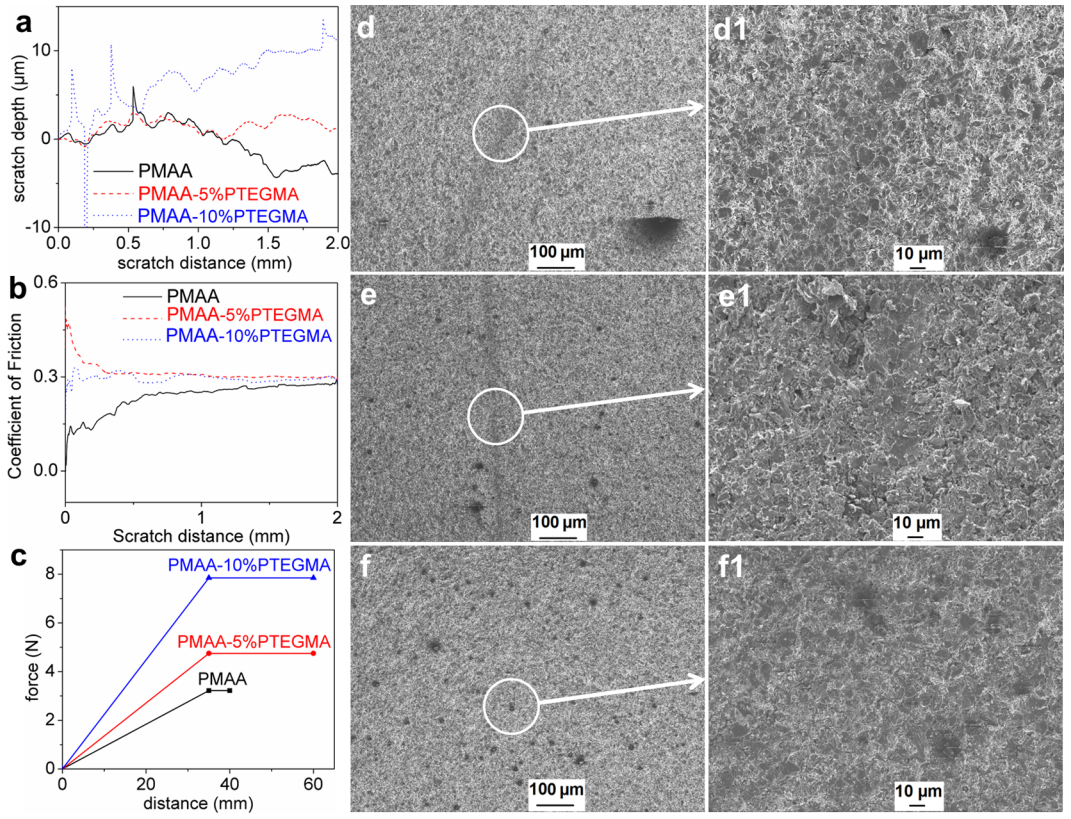

Figure 3. (a) Scratch depth and (b) coefficient of friction vs scratch distance in the scratch test of different PMAA-based binders. (c) Peel test results. (d–f and d1–f1) Scanning electron microscopy images after scratch tests of (d and d1) PMAA, (e and e1) PMAA-5% PTEGMA, and (f and f1) PMAA-10% PTEGMA binders. The scale bars are 100 μm for panels d–f and 10 μm for panels d1–f1.

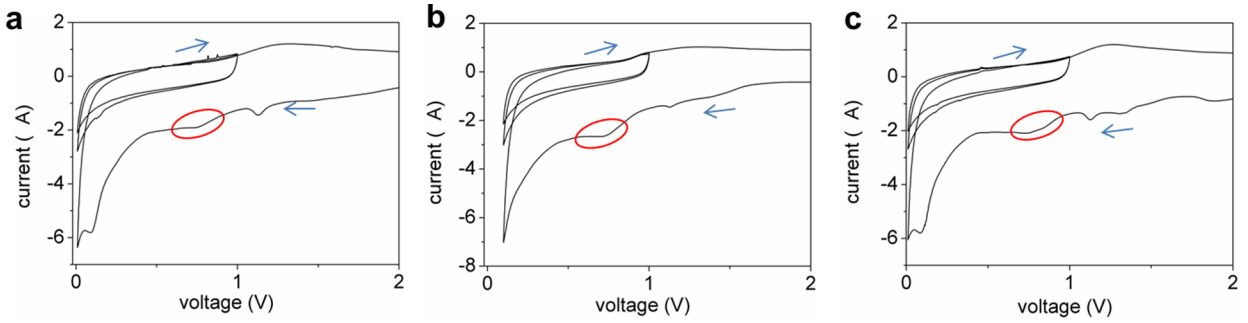

Figure 4. Cyclic voltammetry (CV) of (a) PMAA, (b) PMAA-5% PTEGMA, and (c) PMAA-10% PTEGMA, with the solvent decomposition signals highlighted.

Electrolyte decomposition occurs with both polymers in the first cathodic scan, but no additional current flowed in the voltammogram in the following cycles. All three synthesized polymer binders are electrochemically stable as polymer binders for the negative electrode, considering that the intercalation of lithium into graphite occurs below 0.2 V versus Li/Li$^+$.

The scratch test shown in Figure 3 indicates only the mechanical property of the binder and electrode in a dry state. Polymer binders in an electrode laminate need to be swelled by lithium-ion electrolytes to be ionic conductive, and the electrolyte uptake test was conducted using self-standing polymer samples immersed in the electrolytes. The absolute value of electrolyte uptake is strongly affected by the dimension of the testing sample. The polymer bulk sample is a disk with an area of 3.8 cm^2 and a thickness of ~1 mm. The weight increase after 48 h is shown in Figure 5a, which shows that

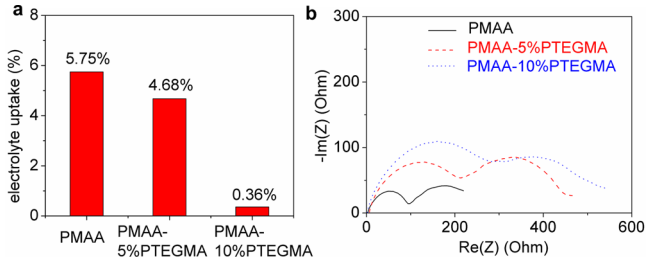

Figure 5. (a) Electrolyte uptake of the polymer binders after 48 h in EC/DEC = 1 and 1 M $LiPF_6$. (b) Cell impedance based on different binders. Impedance was recorded after one cycle at C/25, and the rest were recorded 4 h after half-lithiation in the second cycle.

PMAA has the highest degree of swelling because of the high polarity of the carboxylic acid groups in the polymer backbone.

dx.doi.org/10.1021/am504736y | ACS Appl. Mater. Interfaces 2014, 6, 17111–17118

The level of swelling decreases upon incorporation of the PTEGMA structure, which directly influences the cell impedance shown in Figure 5b. PMAA, with the greatest electrolyte uptake, allows a better ionic conductivity and smaller impedance; incorporation of PTEGMA leads to a smaller level of swelling and higher cell impedance. Although we focus on the influence of binder flexibility, the modification of the polymer structure inevitably changes other relevant properties.

The cycling performance of the different PMAA-based binders is shown in Figure 6a; all the cells were subjected to the formation procedure of C/25 for two cycles and C/10 for five cycles before the long-term 1C cycling. PMAA allows a stable cycling performance of the graphite electrode, which was also shown by others.[22] To further improve the cell performance, the TEG structural moiety in the binder shows an advantage in slow cycling; both 5 and 10% TEG allow a relative higher specific capacity compared to that of the unmodified PMAA binder. The cell gains a reversible capacity of ~320 mAh/g in the formation cycles for PMAA, while with TEG contents, this value is enhanced to ~335 mAh/g. When the cycling rate was increased to 1C, a 5% TEG content seems to be not enough to enhance cell performance, and both PMAA and PMAA-5% PTEGMA show similar performances, with a reversible capacity of ~190 mAh/g at the 1C rate. PMAA-10% PTEGMA, on the other hand, allows a stable cycling at 270 mAh/g at 1C.

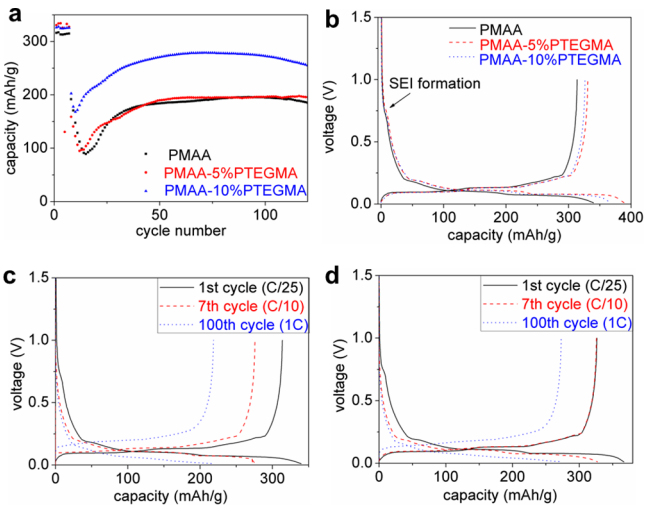

Figure 6. (a) Cycling performance of graphite half-cells with different binders, with C/25 for two cycles, C/10 for five cycles, and then 1C. (b) First-cycle voltage curves. (c) Voltage curves of the electrode with PMAA binder. (d) Voltage curves of the electrode with PMAA-10% PTEGMA binder.

The first cycle voltage curves are shown in Figure 6b; compared to that of PMAA, incorporation of PTEGMA helps to increase the capacity of the graphite anode. The higher capacity and improved rate capability by PTEGMA-containing polymer binder are further corroborated in panels c and d of Figure 6. An ~10% capacity loss is shown from C/25 to C/10 for the PMAA-based cell, although the capacity values are almost the same for PMAA-10% PTEGMA at C/25 and C/10 rates. Note that PMAA-10% PTEGMA shows the largest impedance values in Figure 5b, but this binder allows much-improved cell cycling performance, which further confirms the advantage of a flexible binder.

The microscopic morphologies of the pristine electrodes assembled using the three different binders are shown in panels a–c of Figure 7.[35,36] All the SEM images show similar microstructures, and an appropriate porosity is shown for all the PMAA-based binders with a porosity of ~50%. The graphite particles are uniformly distributed. There is no aggregation of polymer binder. The polymer coating is uniformly coated on the surface of the graphite particle in all cases because of the strong interaction between the carboxylic groups and graphite surface.[4,37] The swelling of the polymer coating by electrolytes allows the good transport of lithium ion between graphite and electrolytes. Panels a1–c1 of Figure 7 show the electrode morphologies after the initial charge–discharge cycle at C/25. A good solid electrolyte interphase must have been formed because a good cycling performance was obtained (Figure 6) with all three different binders, although the SEI is not visible in the SEM images.[38,39] These images indicate a thin SEI, which implies that the PMAA-based

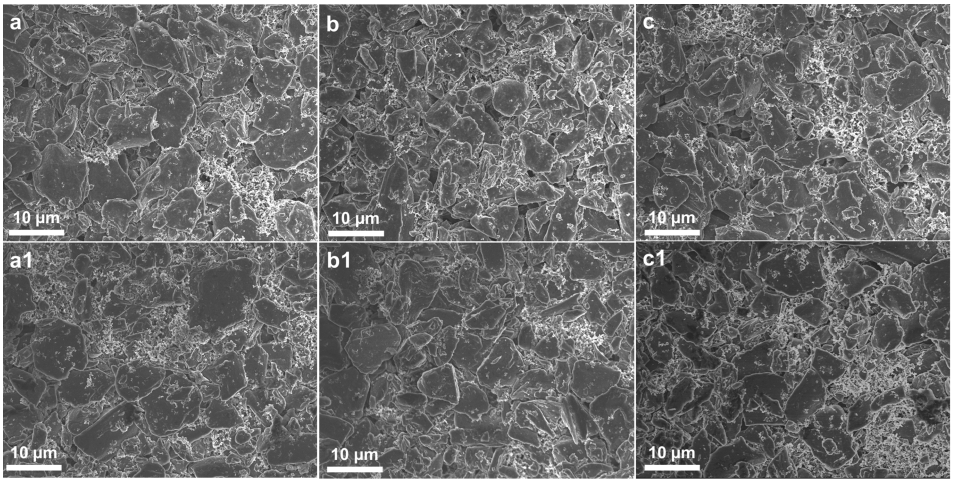

Figure 7. SEM images of graphite electrodes using (a) PMAA before cycling, (a1) PMAA after one cycle, (b) PMAA-5% PTEGMA before cycling, (b1) PMAA-5% PTEGMA after one cycle, (c) PMAA-10% PTEGMA before cycling, and (c1) PMAA-10% PTEGMA after one cycle at C/25. The scale bars are 10 μm.

binders suppress electrolyte decomposition,[22] and this is beneficial for a good electrochemical performance.

The major electrochemical data of the graphite half-cells from the different PMAA-based binders are listed in Table 2.

Table 2. Electrochemical Data of the Graphite Half-Cells with Different PMAA-Based Binders

		PMAA	PMAA-5% PTEGMA	PMAA-10% PTEGMA
first cycle (C/25)	Q_c[a] (mAh/g)	316.3	330.8	326.4
	η[b] (%)	92.09	85.06	88.97
seventh cycle (C/10)	Q_c[a] (mAh/g)	315.1	330.12	325.7
	η[b] (%)	99.61	99.23	99.49
one hundreth cycle (1C)	Q_c[a] (mAh/g)	194.9	196.0	272.9
	η[b] (%)	99.97	99.96	99.96

[a]Charge (delithiation) capacity. [b]Coulombic efficiency.

Although the incorporation of TEG into the polymer binder induces a smaller first-cycle Coulombic efficiency (85.06% for PMAA-5% PTEGMA and 88.97% for PMAA-10% PTEGMA) compared to that of the unmodified PMAA binder (92.09%), the reversible capacity of TEG-based electrodes is higher. At the one hundreth cycle and 1C rate, PMAA-10% PTEGMA allows a reversible capacity of 272.9 mAh/g with a 99.96% CE. PMAA and PMAA-5% PTEGMA, on the other hand, show capacities of ~195 mAh/g.

The enhanced cell performance based on the flexible TEG-containing polymer is explained in Figure 8. Lithiation of the graphite causes an ~10% increase in volume, and polymer binder/AB materials sitting next to these graphite active particles were pushed away in the final lithiated stage; these graphite particles shrink back to the original volume during delithiation process, which induces stress in the electrode laminate. Although the high density of the carboxylic acid functional groups in PMAA facilitates the interfacial interaction between the graphite particle surface and the polymer, they make PMAA a very rigid and brittle structure. It cannot tolerate the stress during excessive cell cycling, and the electrode generates cracks (Figure 8a1), which leads to graphite particle isolation and disintegration of the laminate in the local sites. This explains the weakened electrochemical performance shown in Figure 6.[40] As a well-known flexible structural moiety, the TEG-containing PMAA improves the flexibility of the polymer and avoids crack formation during the handling of the electrode laminate and cell cycling (Figure 8b,b1), resulting in improved cell performance.

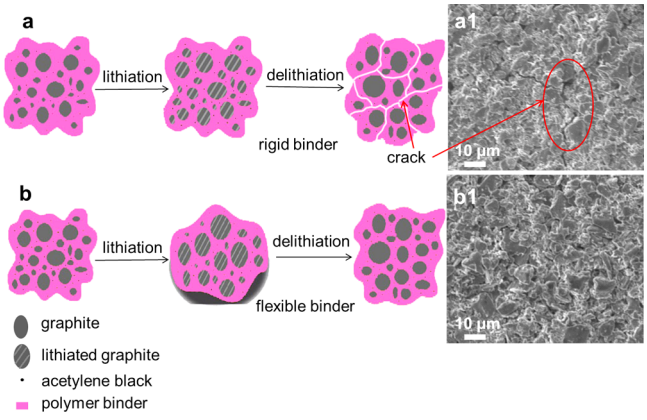

Figure 8. (a) Schematic of rigid binder-based electrodes in the process of Li^+ insertion and extraction. (a1) SEM image of the rigid binder-based graphite electrode after cycling, showing electrode cracking. (b) Schematic of flexible binder-based electrodes in the process of Li^+ insertion and extraction. (b1) SEM image of the flexible binder-based graphite electrode after cycling.

3. CONCLUSIONS

In conclusion, this study demonstrates the systematically varied mechanical properties of an electrode binder and the impact on the electrochemical performance of the electrode. A brittle PMAA was used as a model compound, and the TEG component was introduced for the formation of soft binders to improve the battery performance of the graphite anode in LIBs. The microscratch test demonstrated the different mechanical responses of the electrodes made with different PMAA-based binders. The electrode made with a softer binder can better tolerate the stress exerted by a microscratch. This mechanical response test correlates well with the electrochemical test of the electrode. The electrochemical performance shows that with 10 wt % TEG, enhanced cell cycling performance with a reversible capacity of ~270 mAh/g at 1C was achieved, compared to the value of 190 mAh/g for the unmodified PMAA polymer binder. The origin of the improvement is the improved flexibility of the binder and electrodes, which help inhibit laminate/current collector delamination and particle/particle isolation during lithiation and delithiation of the graphite. This work sheds light on the design of polymer binders in lithium-ion batteries, especially for the high-capacity alloy anodes such as silicon and tin.

■ ASSOCIATED CONTENT

Supporting Information

Details of the characterization of the materials, Fourier transform infrared data of the synthesized binders, and rate performance of the cells. This material is available free of charge via the Internet at http://pubs.acs.org.

■ AUTHOR INFORMATION

Corresponding Author

*E-mail: gliu@lbl.gov. Telephone: (510) 486-7207. Fax: (510) 486-7303.

Author Contributions

N.Y. and H.Z. contributed equally to this work.

Notes

The authors declare no competing financial interest.

■ ACKNOWLEDGMENTS

This work is funded by the Assistant Secretary for Energy Efficiency of the Vehicle Technologies Office of the U.S. Department of Energy, under the Batteries for Advanced Transportation Technologies (BATT) Program. NMR measurements were performed at the Molecular Foundry. Electron microscopy experiments were conducted at the National Center for Electron Microscopy (NCEM). The two facilities are located at Lawrence Berkeley National Laboratory (LBNL) and are supported by the Director Office of Science, Office of Basic Energy Sciences of the U.S. Department of Energy under Contract DE-AC02-05CH11231. N.Y. is grateful for the

funding provided by The Scientific and Technological Research Council of Turkey (TUBITAK) in Ankara, Turkey.

REFERENCES

(1) Gogotsi, Y. Materials Science: Energy Storage Wrapped Up. *Nature* **2014**, *509* (7502), 568−570.

(2) Yuan, W.; Zhao, H.; Hu, H.; Wang, S.; Baker, G. L. Synthesis and Characterization of the Hole-Conducting Silica/Polymer Nanocomposites and Application in Solid-State Dye-Sensitized Solar Cell. *ACS Appl. Mater. Interfaces* **2013**, *5* (10), 4155−4161.

(3) Goodenough, J. B.; Park, K.-S. The Li-Ion Rechargeable Battery: A Perspective. *J. Am. Chem. Soc.* **2013**, *135* (4), 1167−1176.

(4) Zhao, H.; Zhou, X.; Park, S.-J.; Shi, F.; Fu, Y.; Ling, M.; Yuca, N.; Battaglia, V.; Liu, G. A Polymerized Vinylene Carbonate Anode Binder Enhances Performance of Lithium-Ion Batteries. *J. Power Sources* **2014**, *263*, 288−295.

(5) Ling, M.; Qiu, J.; Li, S.; Zhao, H.; Liu, G.; Zhang, S. An Environmentally Benign LIB Fabrication Process Using a Low Cost, Water Soluble and Efficient Binder. *J. Mater. Chem. A* **2013**, *1* (38), 11543−11547.

(6) Li, J.; Dozier, A. K.; Li, Y.; Yang, F.; Cheng, Y.-T. Crack Pattern Formation in Thin Film Lithium-Ion Battery Electrodes. *J. Electrochem. Soc.* **2011**, *158* (6), A689−A694.

(7) Ebner, M.; Marone, F.; Stampanoni, M.; Wood, V. Visualization and Quantification of Electrochemical and Mechanical Degradation in Li Ion Batteries. *Science* **2013**, *342* (6159), 716−720.

(8) Dai, Y.; Cai, L.; White, R. E. Capacity Fade Model for Spinel $LiMn_2O_4$ Electrode. *J. Electrochem. Soc.* **2013**, *160* (1), A182−A190.

(9) Zheng, Z.; Wang, Z.; Song, X.; Xun, S.; Battaglia, V.; Liu, G. Biomimetic Nanostructuring of Copper Thin Films Enhances Adhesion to the Negative Electrode Laminate in Lithium-Ion Batteries. *ChemSusChem* **2014**, DOI: 10.1002/cssc.201402543.

(10) Lee, S.; Oh, E.-S. Performance Enhancement of a Lithium Ion Battery by Incorporation of a Graphene/Polyvinylidene Fluoride Conductive Adhesive Layer Between the Current Collector and The Active Material Layer. *J. Power Sources* **2013**, *244*, 721−725.

(11) Chen, J.; Liu, J.; Qi, Y.; Sun, T.; Li, X. Unveiling the Roles of Binder in the Mechanical Integrity of Electrodes for Lithium-Ion Batteries. *J. Electrochem. Soc.* **2013**, *160* (9), A1502−A1509.

(12) Wang, C.; Wu, H.; Chen, Z.; McDowell, M. T.; Cui, Y.; Bao, Z. Self-Healing Chemistry Enables the Stable Operation of Silicon Microparticle Anodes for High-Energy Lithium-Ion Batteries. *Nat. Chem.* **2013**, *5*, 1042−1048.

(13) Liu, G.; Xun, S.; Vukmirovic, N.; Song, X.; Olalde-Velasco, P.; Zheng, H.; Battaglia, V. S.; Wang, L.; Yang, W. Polymers with Tailored Electronic Structure for High Capacity Lithium Battery Electrodes. *Adv. Mater.* **2011**, *23* (40), 4679−4683.

(14) Xun, S.; Song, X.; Battaglia, V.; Liu, G. Conductive Polymer Binder-Enabled Cycling of Pure Tin Nanoparticle Composite Anode Electrodes for a Lithium-Ion Battery. *J. Electrochem. Soc.* **2013**, *160* (6), A849−A855.

(15) Dai, K.; Zhao, H.; Wang, Z.; Song, X.; Battaglia, V.; Liu, G. Toward High Specific Capacity and High Cycling Stability of Pure Tin Nanoparticles with Conductive Polymer Binder for Sodium Ion Batteries. *J. Power Sources* **2014**, *263*, 276−279.

(16) Li, J.; Klöpsch, R.; Nowak, S.; Kunze, M.; Winter, M.; Passerini, S. Investigations on Cellulose-Based High Voltage Composite Cathodes for Lithium Ion Batteries. *J. Power Sources* **2011**, *196* (18), 7687−7691.

(17) Kim, J.-M.; Park, J.-H.; Lee, C. K.; Lee, S.-Y. Multifunctional Semi-Interpenetrating Polymer Network-Nanoencapsulated Cathode Materials for High-Performance Lithium-Ion Batteries. *Sci. Rep.* **2014**, *4*, 4602.

(18) Hu, L.; La Mantia, F.; Wu, H.; Xie, X.; McDonough, J.; Pasta, M.; Cui, Y. Lithium-Ion Textile Batteries with Large Areal Mass Loading. *Adv. Energy Mater.* **2011**, *1* (6), 1012−1017.

(19) Chen, Z.; Christensen, L.; Dahn, J. R. Large-Volume-Change Electrodes for Li-ion Batteries of Amorphous Alloy Particles Held by Elastomeric Tethers. *Electrochem. Commun.* **2003**, *5* (11), 919−923.

(20) Chen, L.; Xie, X.; Xie, J.; Wang, K.; Yang, J. Binder Effect on Cycling Performance of Silicon/Carbon Composite Anodes for Lithium Ion Batteries. *J. Appl. Electrochem.* **2006**, *36* (10), 1099−1104.

(21) Croce, F.; Appetecchi, G. B.; Persi, L.; Scrosati, B. Nanocomposite Polymer Electrolytes for Lithium Batteries. *Nature* **1998**, *394*, 456−458.

(22) Komaba, S.; Ozeki, T.; Okushi, K. Functional Interface of Polymer Modified Graphite Anode. *J. Power Sources* **2009**, *189*, 197−203.

(23) Erk, C.; Brezesinski, T.; Sommer, H.; Schneider, R.; Janek, J. Toward Silicon Anodes for Next-Generation Lithium Ion Batteries: A Comparative Performance Study of Various Polymer Binders and Silicon Nanopowders. *ACS Appl. Mater. Interfaces* **2013**, *5* (15), 7299−7307.

(24) Magasinski, A.; Zdyrko, B.; Kovalenko, I.; Hertzberg, B.; Burtovyy, R.; Huebner, C. F.; Fuller, T. F.; Luzinov, I.; Yushin, G. Toward Efficient Binders for Li-Ion Battery Si-Based Anodes: Polyacrylic Acid. *ACS Appl. Mater. Interfaces* **2010**, *2* (11), 3004−3010.

(25) Yoshio, M.; Brodd, R. J.; Kozawa, A. *Lithium Ion Batteries: Science and Technologies*; Springer: Berlin, 2009.

(26) Armand, M. B.; Chabagno, J. M.; Duclot, M. Poly-ethers as Solid Electrolytes. Second International Meeting on Solid Electrolytes, St Andrew, Scotland, September 20−22, 1978.

(27) Jia, Z.; Yuan, W.; Zhao, H.; Hu, H.; Baker, G. L. Composite Electrolytes Comprised of Poly(Ethylene Oxide) and Silica Nanoparticles with Grafted Poly(Ethylene Oxide)-Containing Polymers. *RSC Adv.* **2014**, DOI: 10.1039/C4RA07262F.

(28) Wu, M.; Xiao, X.; Vukmirovic, N.; Xun, S.; Das, P. K.; Song, X.; Olalde-Velasco, P.; Wang, D.; Weber, A. Z.; Wang, L.-W.; Battaglia, V. S.; Yang, W.; Liu, G. Toward an Ideal Polymer Binder Design for High-Capacity Battery Anodes. *J. Am. Chem. Soc.* **2013**, *135* (32), 12048−12056.

(29) Xiao, X.; Xie, T.; Cheng, Y.-T. Self-Healable Graphene Polymer Composites. *J. Mater. Chem.* **2010**, *20* (17), 3508−3514.

(30) Wu, H.; Cui, Y. Designing Nanostructured Si Anodes for High Energy Lithium Ion Batteries. *Nano Today* **2012**, *7* (5), 414−429.

(31) Hu, H.; Yuan, W.; Lu, L.; Zhao, H.; Jia, Z.; Baker, G. L. Low Glass Transition Temperature Polymer Electrolyte Prepared From Ionic Liquid Grafted Polyethylene Oxide. *J. Polym. Sci., Part A: Polym. Chem.* **2014**, *52* (15), 2104−2110.

(32) Hu, H.; Yuan, W.; Zhao, H.; Baker, G. L.; Novel, A. Polymer Gel Electrolyte: Direct Polymerization of Ionic Liquid From Surface of Silica Nanoparticles. *J. Polym. Sci., Part A: Polym. Chem.* **2014**, *52* (1), 121−127.

(33) Su, X.; Wu, Q.; Li, J.; Xiao, X.; Lott, A.; Lu, W.; Sheldon, B. W.; Wu, J. Silicon-Based Nanomaterials for Lithium-Ion Batteries: A Review. *Adv. Energy Mater.* **2014**, *4* (1), DOI: 10.1002/aenm.201300882.

(34) Ryou, M.-H.; Kim, J.; Lee, I.; Kim, S.; Jeong, Y. K.; Hong, S.; Ryu, J. H.; Kim, T.-S.; Park, J.-K.; Lee, H.; Choi, J. W. Mussel-Inspired Adhesive Binders for High-Performance Silicon Nanoparticle Anodes in Lithium-Ion Batteries. *Adv. Mater.* **2013**, *25* (11), 1571−1576.

(35) Qin, J.; Zhao, H.; Zhu, R.; Zhang, X.; Gu, Y. Effect of Chemical Interaction on Morphology and Mechanical Properties of CPI-OH/SiO_2 Hybrid Films with Coupling Agent. *J. Appl. Polym. Sci.* **2007**, *104* (6), 3530−3538.

(36) Qin, J.; Zhao, H.; Liu, X.; Zhang, X.; Gu, Y. Double Phase Separation in Preparing Polyimide/Silica Hybrid Films by Sol−Gel Method. *Polymer* **2007**, *48* (12), 3379−3383.

(37) Guerfi, A.; Kaneko, M.; Petitclerc, M.; Mori, M.; Zaghib, K. $LiFePO_4$ water-soluble binder electrode for Li-ion batteries. *J. Power Sources* **2007**, *163* (2), 1047−1052.

(38) Zhao, H.; Park, S.-J.; Shi, F.; Fu, Y.; Battaglia, V.; Ross, P. N.; Liu, G. Propylene Carbonate (PC)-Based Electrolytes with High Coulombic Efficiency for Lithium-Ion Batteries. *J. Electrochem. Soc.* **2014**, *161* (1), A194−A200.

(39) Shi, F.; Zhao, H.; Liu, G.; Ross, P. N.; Somorjai, G. A.; Komvopoulos, K. Identification of Diethyl 2,5-Dioxahexane Dicarboxylate and Polyethylene Carbonate as Decomposition Products of

Ethylene Carbonate Based Electrolytes by Fourier Transform Infrared Spectroscopy. *J. Phys. Chem. C* **2014**, *118* (27), 14732−14738.
(40) Dai, Y.; Cai, L.; White, R. E. Simulation and Analysis of Inhomogeneous Degradation in Large Format $LiMn_2O_4$/Carbon Cells. *J. Electrochem. Soc.* **2014**, *161* (8), E3348−E3356.